Journal of Materials Engineering and Performance
ASM INTERNATIONAL

Fabrication of silicon nanowire forests for thermoelectric applications by Metal-Assisted Chemical Etching

Journal:	*Journal of Materials Engineering and Performance*
Manuscript ID	Draft
Manuscript Type:	Technical Paper
Date Submitted by the Author:	n/a
Complete List of Authors:	Dimaggio, Elisabetta; University of Pisa, Dipartimento di Ingegneria dell'Informazione Narducci, Dario; University of Milan – Bicocca , Materials Science Pennelli, Giovanni; University of Pisa, Dipartimento di Ingegneria dell'Informazione; University of Pisa
Keywords:	thermoelectricity, silicon nanowires, Metal assisted chemical etching

Fabrication of silicon nanowire forests for thermoelectric applications by Metal-Assisted Chemical Etching

Elisabetta Dimaggio[1], Dario Narducci[2], Giovanni Pennelli[1]
1. Dipartimento di Ingegneria dell'Informazione, Universita' di Pisa
Via G.Caruso16, I-56122 PISA
2. Dipartimento di Scienza dei Materiali, Universita' di Milano Bicocca
Via R. Cozzi 55, I-20125 Milano

Abstract

Silicon nanowires, whose thermal conductivity is strongly reduced with respect to that of the bulk silicon, are very promising for high efficient thermoelectric conversion.
Our work is focused on the development of a technique for the fabrication of thermoelectric generators which are based on vertical silicon nanowire forests, achieved through a metal-assisted chemical etch. As heavily doped nanowires are essential in thermoelectric applications, we have applied this chemical process both on lightly and on highly doped silicon substrates. Comparing the results, we have found that the etch behaves in a completely distinct way when applied to the differently doped substrates.
We report here the results of this comparison, giving a preliminary insight to the diverse behavior occurred. We found that the different initial nucleation of silver, which determines the hole injection essential to the etching of silicon, is the key point of this different behavior.

Introduction

Crystalline silicon nanostructures show excellent thermoelectric properties. Indeed, both the Seebeck coefficient and the electrical conductivity depend on the carrier concentration, which can be tailored by means of well assessed doping processes in order to achieve interesting values for thermoelectric applications. The thermal conductivity, which is very high in bulk silicon (148 W/(mK)), is reduced down to few W/(mK) in nanostrucures, such as nanowires, due to the scattering of phonons on the nanowire walls[1,4]. Hence, thermoelectric generator devices (TGs), based on a large number of silicon nanostructures, could potentially reach high thermal to electrical conversion efficiencies. High resolution lithography, combined with standard silicon processing, can be exploited for the fabrication of large arrays of interconnected nanowires[5,6]. Unfortunately, these techniques, based on advanced lithography, are very expensive. Hence, they can be implemented only for the fabrication of small TGs, which can be used for energy scavenging and/or for supplying integrated circuits/small sensor nodes. Low-cost techniques for the fabrication of a huge number of interconnected nanowires need to be developed for a considerable production of electrical power. A possibility is to exploit the Metal Assisted Chemical Etching[7,9] (MACE), which allows the fabrication of vertical structures (nanowires) with high aspect ratio. Figure 1

shows a cross section of a silicon chip, etched by MACE (5:16:60 $AgNO_3$ (0.1 N):HF(48%):) for 4h: a forest of more than 10^7 silicon nanowires/mm^2, with an average diameter of 80 nm and more than 75 um long, has been obtained. The sketch in the figure represents a possible thermoelectric module based on (at least) two nanowire forests, respectively *p* and *n* heavily doped. The top end of the nanowires can be contacted through a copper layer, which can be grown by electrodeposition, as previously reported[10]. The bottom end of the nanowires are connected together through the silicon substrate, whose thermal and electrical conduction is in series with that of the nanowires. From the thermal point of view, the conductivity of the nanowires is reduced, meanwhile the conductivity of the bulk silicon substrate is very high, and thus it has only a negligible influence on the heat conduction. From the electrical point of view, the conductivity of the nanowire forest can be tailored (strongly increased) by standard silicon doping processes (diffusion), which can be implemented after MACE etching. However, the resistance of the substrate still depends on its original doping concentration. The main target of this paper is to report on the application of the MACE technique on silicon substrates with different *n*-doping concentrations. In particular, we tested MACE with several concentration ratios of silver and hydrofluoric acid, on lightly and heavily *n*-doped substrates (see section II), reporting a substantial different behavior. A possible interpretation (see section III) can be found in the different initial nucleation of Silver on the silicon surface.

FIGURE_N1

FIGURE 1: photo of a silicon nanowire forest. In the inset: a sketch of a thermoelectric generator module, based on nanowire forests, doped *n*+ and *p*+.

Metal Assisted Chemical Etching of *n* and *n*+ substrates.

FIGURE_N2

FIGURE 2. One-step MACE on a *n*-doped substrate (5-10 Ohm cm, doping between $5X10^{14}$ cm^{-3} and 10^{15} cm^{-3}), for several [HF]/[$AgNO_3$] concentrations. The triangular diagram on the top shows the tested concentration ratios. Results after 30 min of etching time are shown in the SEM images on the bottom.

Metal Assisted Chemical Etching is based on the deposition of metal nanoparticles (in general Silver or Gold) on a silicon surface, followed by an etch in an aqueous solution containing both an

oxidizing component and a complexing component such as Hydrofluoric Acid (HF). Following the most common explanations of MACE[11,15], the metal nanoparticles act as catalyst for the local oxidation of silicon, which is then removed by HF. Before the oxidizing etching, metal nanoparticles can be deposited by several techniques, such as thermal evaporation followed by an annealing procedure, or by the reduction of a metal salt in a suitable solution. The latter deposition technique is at the basis of the "two-steps" procedure, because it consists in soaking the silicon substrate at first in a solution with the metal salt, leading to the formation of the nanoparticles, and then in a solution containing an oxidizing agent, such as hydrogen peroxide, together with hydrofluoric acid to perform the etch. The reaction proceeds locally under the deposited metal nanoparticles, which soak into the silicon, digging very deep holes. The etch is highly directional (vertical), and thus, at the end, vertical silicon pillars (nanowires) remain defined among the deep holes. Alternatively, a "one-step" procedure can be applied. It consists in soaking the silicon substrate in one solution only, containing both a metal salt, such as silver nitrate ($AgNO_3$), and HF. Nanoparticles are produced when silver is reduced, withdrawing electrons from silicon. This is equivalent to say that holes are injected into the silicon, which is thus locally oxidized and then removed by HF etching. We found that this "one-step" procedure is more reliable, and in particular it allows the fabrication of silicon nanowires with higher aspect ratio with respect to that achievable with the "two-steps" procedure. As long nanowires are more suitable for thermoelectric applications, we focused on the "one-step" procedure.

The localized hole injection/silicon etching is the more accredited mechanism for the etching, both in the case of the two-steps and of the one-step procedure. However, especially for the one-step procedure, the exact role of the etching parameters, and in particular the role of the doping of the silicon substrate, has not been clearly established yet. Certainly, the effect of the concentration ratio between the oxidizing and complexing reagents is important; its effect on the etch has been largely investigated for the two-steps[15-18] process ($[HF]/[H_2O_2]$ ratio). In the case of the one-step[20] process, the effect of the $[HF]/[AgNO_3]$ concentration ratio is less documented. For this reason, we

tested the one-step MACE procedure with different [HF]/[$AgNO_3$] ratios (in deionized water), on both *n*- and *n*+-doped substrates. The $AgNO_3$ concentration determines the rate of hole injection, meanwhile the HF concentration determines the silicon etch rate.

Figure 2 refers to the etch tests performed on a phosphorous-doped (*n*-doped) substrate, whose resistivity is 5-10 Ohm cm, which means a phosphorous doping concentration between 4×10^{14} and 10^{15} cm^{-3}. The investigated [HF]/[$AgNO_3$] concentration ratios have been reported on the triangular diagram shown on the top of Figure 2. All the etches have been performed for the same time (30 minutes) at a temperature of about 17 °C (± 2 °C). As a result of the etching process, the samples appear covered by a grey powder, characteristic of polycrystalline silver. It is sufficient to soak the samples in HNO_3:H_2O 1:1 solution for 2 minute for removing all the silver powder deposited on them. Then, morphological characterization has been performed by SEM imaging. The SEM images inserted in the bottom of Figure 2 show the cross sections of the samples achieved with the tested concentration ratios. Not all the concentration ratios yield vertical silicon structures: in some cases the surface resulted uniformly etched (polished). The length of the nanowires, measured by SEM images, has been reported on the triangular diagram for each concentration ratio; the 0 value means uniform etching (polishing, no nanowires). The reagent concentrations, concentration ratios and the nanowire lengths are also reported in Table 1 for clarity.

Table 1: tested HF and $AgNO_3$ concentrations, concentration ratios and resulted nanowire lengths.

Number	[HF] (mol/l)	[$AgNO_3$] (mol/l)	[HF]/[$AgNO_3$]	n doping length (um)	n+ doping length (um)
1	0.00116	2.0×10^{-5}	58.2	POLISHING	POLISHING
2	0.00372	5.0×10^{-5}	74.50	POLISHING	4e-6
3	0.00436	3.1×10^{-5}	139.7	15	POLISHING
4	0.00931	3×10^{-5}	310.4	30	POLISHING
5	0.00582	1.3×10^{-5}	447.7	3.5	POLISHING
6	0.00465	6.0×10^{-5}	776.1	5	POLISHING
7	0.00698	6.0×10^{-5}	1164.1	10	POLISHING
8	0.01397	1.0×10^{-5}	1396.9	50	POLISHING

In the case of low concentration ratios (case 1 and 2) the surface resulted uniformly etched. A possible explanation can be that the rate of the hole injection is higher with respect to the HF

etching rate: there are too much holes and the rate of the oxidized silicon etching is too low. Therefore, holes have time to diffuse on all the surface, resulting in a uniform etching. Hence, vertical silicon structures do not result defined. For the cases from 3 to 8 nanowires are formed, and tendentially their length increases with the increasing of the [HF]/[$AgNO_3$] ratio. It must be noted that the average diameter of the nanowires, which is about 80 nm, is almost the same for all the samples (case 3 to 8).

FIGURE_N3

FIGURE 3. One-step MACE on a n+-doped substrate (resistivity 0.003 Ohm cm, doping between $5X10^{14}$ cm^{-3} and 10^{15} cm^{-3}), for several [HF]/[$AgNO_3$] concentrations. The triangular diagram on the top shows the tested concentration ratios. Results after 30 min of etching time are shown in the SEM images on the bottom.

Figure 3 refers to the etch tests performed on n^+-doped substrates, whose resistivity is 0.003 Ohm cm, which corresponds to an Arsenic doping concentration of $5X10^{19}$. The tested [HF]//[$AgNO_3$] concentration ratios are the same of that of the *n*-doped substrates, as reported on the triangular diagram on top of the Figure 3. The SEM images on the bottom of Figure 3 show the samples achieved after 30 min etching and cleaning in HNO_3: H_2O 1:1 solution for 2 minute (for removing the deposited silver). In most cases we found a uniform etching of the surface, with very few nanowires placed at random. Only in one case we found a quite uniform nanowire forest with nanowires 4 μm long. However, these nanowires resulted porous. In all cases, a layer of porous silicon is formed under the surface. We concluded that no good nanowire forest, made of monocrystalline silicon nanowires, can be fabricated on n^+ (heavily doped) silicon substrates, at least in the explored ranges of parameters (reagent concentrations). To be noted that also the two-steps procedure does not give good nanowire forests on heavily doped substrates[19]. We recall that the thermoelectric applications of these forests require a heavily doped substrate, in order to minimize its electrical resistance which is in series with that of the nanowires. On the other hand, even though porous nanowires can be eventually fabricated on $n+$ substrates, their electrical resistance will be very high, making them unsuitable for thermoelectric applications.

Preliminary discussion and interpretation of the results.

Several interpretations have been proposed for the explanation of the MACE etching, both for the two-steps and the one-step technique. In particular, for the latter technique, a suitable model for the full comprehension of the etching mechanism, which justifies the different behavior on moderately doped and on heavily doped substrates, still need to be developed. For sure, one-step MACE is driven by at least two different phenomena: hole injection due to the reduction of silver and HF localized silicon oxide etching. These two phenomena are clearly strictly related. However, from the experimental results, it is reasonable to affirm that the silicon oxidation is driven by the hole injection, due to silver reduction. The development of an exhaustive model is beyond the scope of the present work. However, we made some trials to give some preliminary insights to the first of these two phenomena (silver reduction). Essentially, we have investigated: 1) the possible influence that the type of silver salt could have on the etching; 2) the morphology of the initial sedimentation of the silver particles on the silicon substrate.

1) We performed most of our trials with silver nitrate ($AgNO_3$). In order to exclude any possible effect of the counterion (NO_3^-), we also performed some trials using silver sulfate (Ag_2SO_4) as oxidizing agent. We compared the results with those achieved by $AgNO_3$, and we did not note any significant difference using concentration ratios with the right proportion (half molar concentration of Ag_2SO_4 with respect to that of $AgNO_3$). We concluded that only silver plays a role in the MACE etching.

2) We tried to give an insight on the mechanism of the silver deposition onto the silicon substrate, and also on the progression of the etch. To this end, we performed etches with the same solution (5:16:60 $AgNO_3$(0.1 M): HF(48%):H_2O) for increasing times, starting from 10 s, both on *n* and *n*+ silicon substrate. After the etching, we made a morphological characterization of the Silver nanoparticles deposited on the silicon substrate. Figure 4 shows several SEM images, taken after MACE etching for 10, 20 and 30 s.

FIGURE_N4

FIGURE 4. Silver seeds deposited on silicon substrates after 10", 20" and 30" of MACE etching (CONCENTRATION). On the top: n-doped substrate (resistivity 5-10 Ohm cm); on the bottom: n+-doped substrate (resistivity 0.003 Ohm cm).

The sequence of three images on the top is related to the etching of n-doped substrates (as before, resistivity 5-10 Ohm cm); they are compared with the three images of the sequence on the bottom, obtained on *n*+-doped substrates (resistivity 0.003 Ohm cm). In both sequences it is evident the sedimentation of silver on the silicon substrate: these silver "seeds" are the starting points of the etch. However, comparing the SEM images it is clearly visible that the silver seeds are different for *n* and *n*+ substrates, both as surface concentration and as shape and average diameter. In particular, on the *n*-doped substrate silver is at first deposited as islands which seem to be partially interconnected; areas of free silicon are visible in between. On the 20 s image (middle) the thickness on the isles is increased, but still areas of free silicon are visible in between. In the 30 s image (third on the top), dendritic structures are grown starting from a few silver nanoparticles. It must be noted that for very long etches (30 minutes or more) the sample is fully covered by silver, organized in these dendritic structures. The behavior is completely different on the *n*+-doped substrate. After 10 s etching, the silicon surface appears covered by silver nanoparticles, which are smaller with respect to that of the *n*-doped substrate but which fully cover the silicon surface and no free silicon spaces are visible. After 20 s of etch, the dendritic structures have already begun to grow, and they result strongly increased after 30 s etch.

The comparison of these SEM images suggests that the etch is localized in the case of n-doped substrate, because it proceeds under the silicon nanoparticles and it is ineffective on the free silicon areas, between the silver seeds. Instead, in the case of *n*+-doped substrate, silver nanoparticles cover all the silicon surface. Hence, the surface is uniformly etched and nanowires are not defined. This is confirmed by the AFM images of the silicon surfaces, shown in Figure 5. After 30 s of etching time (*n*-doped substrate on the left, *n*+-doped substrate on the right), silver has been removed from the silicon substrate with a 2 minutes etching in 1:1 HNO_3:H_2O, as previously reported. Then, AFM images of the bare silicon surfaces have been taken in no-contact mode. The left image, related to the *n*-doped substrate, shows the beginning of the formation of silicon

nanowires (after 30 s etch): almost vertical structures few tens of nanometers tall (30-50 nm) are visible. At this stage, it is not possible to give a precise measurement of the nanowire length, which corresponds to the depth of the holes. In the case of the *n*+ substrate (AFM image on the right) only a rough surface is obtained; the standard deviation of the roughness has been measured by AFM imaging analysis, performed by Gwyddion software, and it resulted of about 4 nm.

FIGURE_N5

FIGURE 5. AFM images (no-contact mode) of silicon surfaces, after 30" of MACE etching and silver removal by HNO3 etching (see text). On the left: the n-doped substrate shows the initial formation of vertical structures, whose length can be estimated of 30-50 nm. On the right: the n+-doped substrate presents a rough surface, with a standard deviation of about 4 nm.

From these SEM and AFM imaging of the initial phase of the etching, we suggest that the initial sedimentation of silver, which is different on *n*-doped and *n*+-doped substrates, plays an important role in the Metal Assisted Chemical Etching.

A possible interpretation must take into account the chemical potential of the solution, given by the $AgNO_3$ concentration, and of the silicon substrate, determined by the doping concentration [7,21,22]. For low doping values, a Schottky barrier is formed at the silicon-solution interface, and it prevents the injection of holes into the silicon substrate. Therefore, etch does not proceed on the areas of free silicon. Initially, silver reduction occurs close to defects on the surface, and then these silver seeds act as hole injection sites because there is not barrier for holes at the silicon-silver interface. The etch proceeds under the nanoparticles, or very close to them, where holes are injected. This phenomenon is driven by the reduction, and hence the deposition, of silver from the solution. It is well visible in the third image on the top of Figure 4, related to the *n*-doped substrate etched for 30 s, that silver nanoparticles are sank into the silicon, meanwile free areas are practically unetched. Silver is deposited not just onto the nanoparticle, but it increases the dendritic structures which start only from a few sites, which were speculated to be caused by diffusion-limited aggregation[11]. Therefore, for the selectivity of the etch, it is fundamental the presence of a Schottky barrier in free silicon areas, which is instead lowered to the silicon-Ag interface.

It is well known that Schottky metal/silicon contacts have always an ohmic behavior on heavily doped silicon, because even if a barrier is generated at the interface, it is very thin and carrier

injection can easily happen by tunneling. Almost any metal, deposited on a heavily doped silicon substrate, shows an ohmic (not rectifying) behavior. Even if the mechanism of the etch on heavily doped substrates is similar (Ag reduction injects holes, oxidized silicon is removed by HF), there is not any barrier effect between silicon and solution, which is necessary for the selectivity of the etch. Therefore, at firs the hole injection is not localized anymore and hence all the surface is etched, and moreover a larger amount of holes is injected into the silicon, so that porous structures are formed.

Conclusions

We reported on a fabrication process based on MACE etching, which allows the production, on large-scale and with low-cost, of vertical silicon nanowires (silicon nanowire forests). Once doped, interconnected and assembled, these nanowire forests, which have a very small thermal conductivity, can be used for high efficient thermoelectric generation. We discussed the MACE etching of silicon substrates *n* and *n*+ doped, showing that it is very difficult to achieve crystalline nanowire forests on heavily doped silicon. We presented some trials to give a preliminary insights to the silver sedimentation on the silicon surface, concluding that, in the case of the *n*+ substrates, a full coverage of silicon occurs just at the very beginning of the etch. This brings to a rough surface uniformly etched, without any formation of vertical nanowires.

Bibliography

[1] D. Li, Y. Wu, P. Kim, L. Shi, P. Yang, A. Majumdar, *Thermal conductivity of individual silicon nanowires*, Appl. Phys. Lett. 83 (14) (2003) 2934–2936.
[2] J. Lim, K. Hippalgaonkar, S. Andrews, C., A. Majumdar, P. Yang, Q*uantifying surface roughness effects on phonon transport in silicon nanowires*, Nano Letters 12 (5) (2012) 2475–2482.
[3] J. Feser, J. Sadhu, B. Azeredo, H. Hsu, J. Ma, J. Kim, M. Seong, N. Fang, X. Li, P. Ferreira, S. Sinha, D. Cahill, *Thermal conductivity of silicon nanowire arrays with controlled roughness*, J. Appl. Phys. 112 (2012) 114306.
[4] G. Pennelli, A. Nannini, M. Macucci, *Indirect measurement of thermal conductivity in silicon nanowires*, J. Appl. Phys. 115 (2014) 084507.
[5] G. Pennelli, M. Totaro, M. Piotto, P. Bruschi, *Seebeck coefficient of nanowires interconnected into large area networks*, Nano Lett. 13 (2013) 2592.
[6] G.Pennelli, M.Macucci, *High-power thermoelectric generators based on nanostructured silicon*, Semicond. Sci. Technol. 31 (2016) 054001.
[7] Z. Huang, N. Geyer, P. Werner, J. De Boor, U. Gosele, *Metal-assisted chemical etching of silicon: a review*, Advanced materials 23 (2) (2011) 285–308.
[8] M. Li, Y. Li, W. Liu, L. Yue, R. Li, Y. Luo, M. Trevor, B. Jiang, F. Bai, P. Fu, Y. Zhao, C. Shen, J. M. Mbengue, *Metal-assisted chemical etching for designable monocrystalline silicon nanostructure*, Materials Research Bulletin 76 (2016) 436.
[9] M. Bollani, J. Osmond, G. Nicotra, C. Spinella, D.Narducci, *Strain-induced generation of silicon nanopillars*, Nanotechnology 24 (2013) 335302.

[10] E. Dimaggio, G. Pennelli, *Reliable fabrication of metal contacts on silicon nanowire forests*, Nano Letters 7 (2016) 4348.
[11] Z. R. Smith, R. L. Smith, S. D. Collins, *Mechanism of nanowire formation in metal assisted chemical etching*, Electrochimica Acta 92 (2013), 139.
[12] K. Peng, Y. Yan, S. Gao, J. Zhu, *Dendrite-Assisted Growth of Silicon Nanowires in Electroless Metal Deposition*, Adv. Funct. Mater. 13 (2003) 127.
[13] C. Chartier, S. Bastide, C.Lévy-Clément, *Metal-assisted chemical etching of silicon in HF–H_2O_2*, Electrochimica Acta 53 (2008) 5509.
[14] K. W. Kolasinski, *The mechanism of galvanic/metal-assisted etching of silicon,* Nanoscale Research Letters 9 (2014) 432. (HF/H2O2)
[15] J. Kim, H. Han, Y. H.Kim, S.-H. Choi, J.-C. Kim, W. Lee, *Au/Ag Bilayered Metal Mesh as a Si Etching Catalyst for Controlled Fabrication of Si Nanowires,* ACS Nano 5 (2011) 3222.
[16] L. Li, Y. Liu, X. Zhao, Z. Lin, C.-P. Wong, *Uniform Vertical Trench Etching on Silicon with High Aspect Ratio by Metal-Assisted Chemical Etching Using Nanoporous Catalysts*, ACS Appl. Mater. Interfaces 6, (2014) 575.
[17] K. Tsujino, M. Matsumura, *Morphology of nanoholes formed in silicon by wet etching in solutions containing HF and H 2 O 2 at different concentrations using silver nanoparticles as catalysts*, Electrochimica Acta 53 (2007) 28.
[18] M.-L. Zhang, K.-Q. Peng, X. Fan, J.-S. Jie, R.-Q. Zhang, S.-T. Lee, N.-B. Wong, *Preparation of Large-Area Uniform Silicon Nanowires Arrays through Metal-Assisted Chemical Etching* J. Phys. Chem. C 112 (2008) 4444.
[19] K. Peng, H. Fang, J. Hu, Y. Wu, J. Zhu,Y.Yan, S.T. Lee *Metal-Particle-Induced, Highly Localized Site-Specific Etching of Si and Formation of Single-Crystalline Si Nanowires in Aqueous Fluoride Solution* Chem. Eur. J. 12 (2006), 7942.
[20] Y. Qi, Z. Wang, M. Zhang, F. Yang, X. Wang, *A Processing Window for Fabricating Heavily Doped Silicon Nanowires by Metal-Assisted Chemical Etching,* J. Phys. Chem. C 117 (2013) 25090.
[21] S J Rezvani, R. Gunnella, D. Neilson, L. Boarino, L. Croin, G Aprile, M. Fretto, P. Rizzi, D. Antonioli, N. Pinto, *Effect of carrier tunneling on the structure of Si nanowires fabricated by metal assisted etching* Nanotechnology 27 (2016) 345301.
[22] X.Li, Y. Xiao, C. Yan, K. Zhou, S. L. Schweizer, A. Sprafke, J.-H. Lee, R. B. Wehrspohn, I*nfluence of the Mobility of Pt Nanoparticles on the Anisotropic Etching Properties of Silicon*, ECS Solid State Letters, 2 (2013) 22.

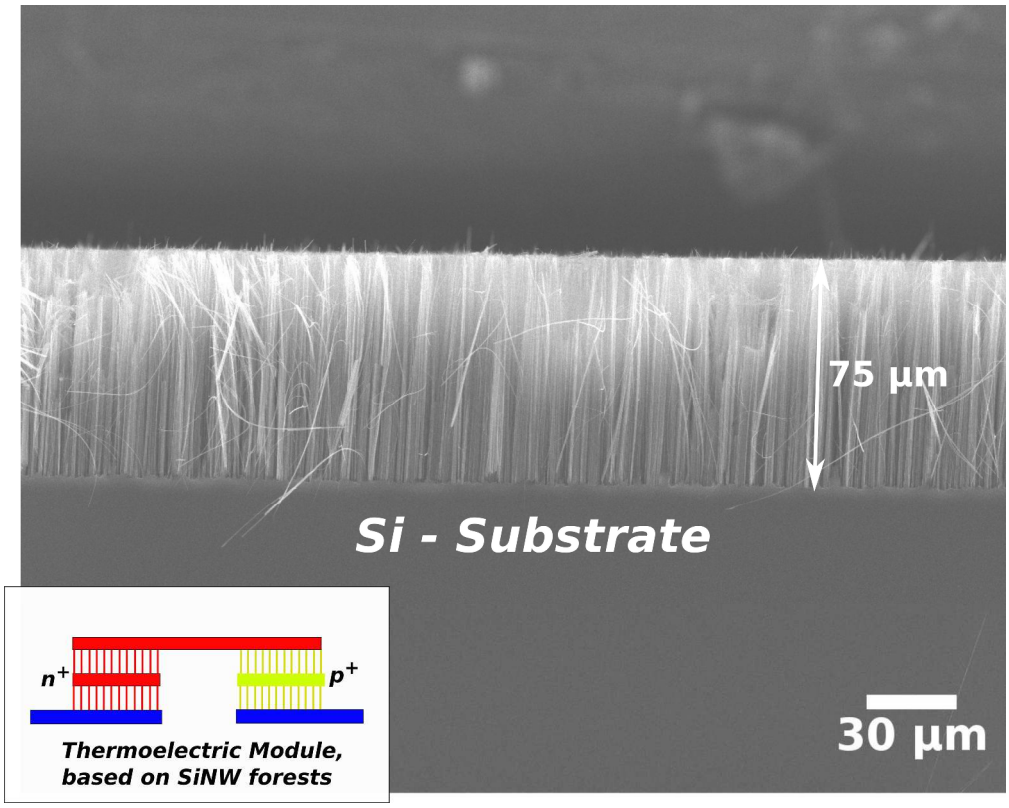

Figure 1. Photo of a silicon nanowire forest. In the inset: a sketch of a thermoelectric generator module, based on nanowire forests, doped n+ and p+.

367x292mm (300 x 300 DPI)

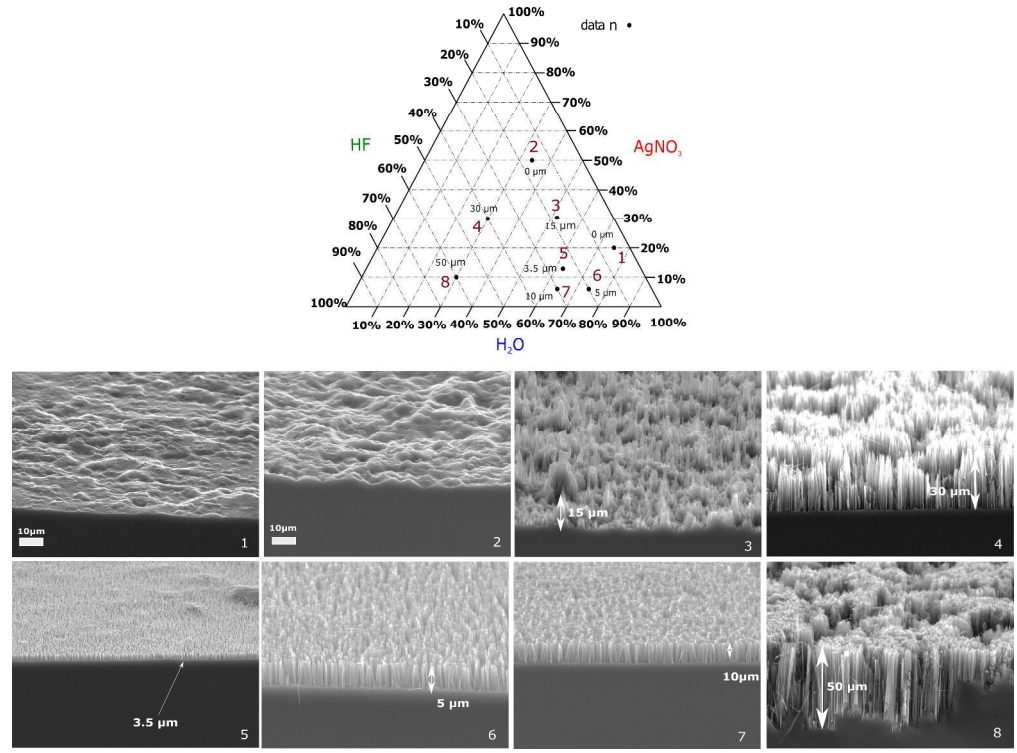

Figure 2. One-step MACE on a n-doped substrate (5-10 Ohm cm, doping between 5X1014 cm-3 and 1015 cm-3), for several [HF]/[AgNO3] concentrations. The triangular diagram on the top shows the tested concentration ratios. Results after 30 min of etching time are shown in the SEM images on the bottom.

1291x957mm (96 x 96 DPI)

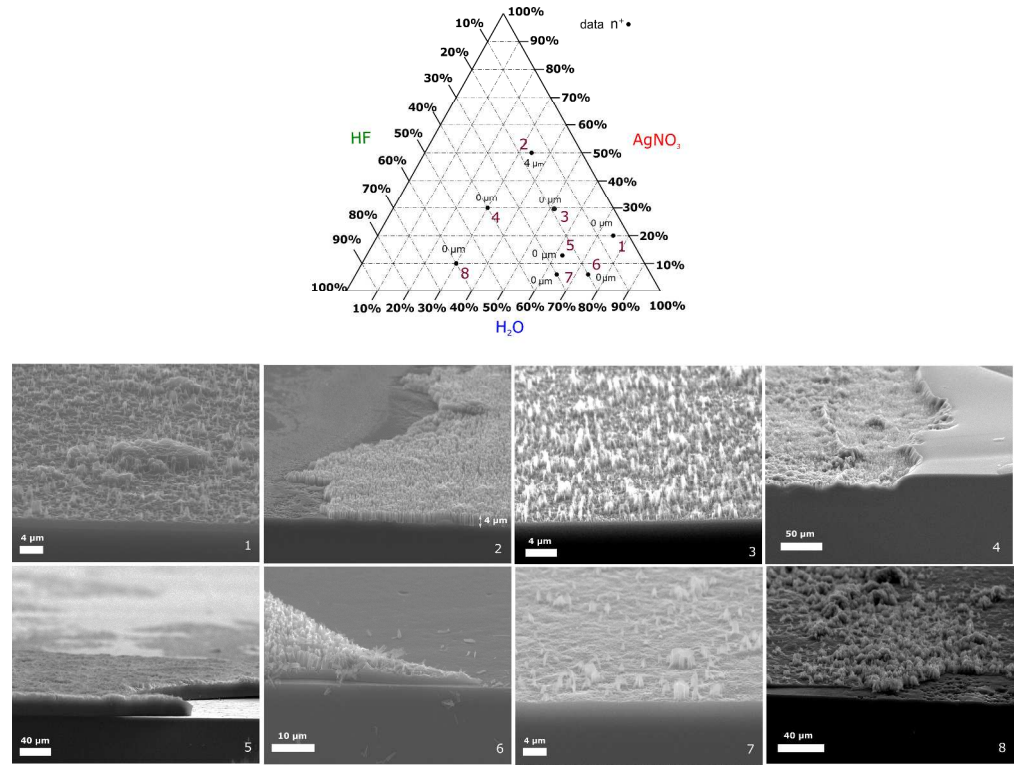

Figure 3. One-step MACE on a n+-doped substrate (resistivity 0.003 Ohm cm, doping between 5X1014 cm-3 and 1015 cm-3), for several [HF]/[AgNO3] concentrations. The triangular diagram on the top shows the tested concentration ratios. Results after 30 min of etching time are shown in the SEM images on the bottom.

1371x1036mm (96 x 96 DPI)

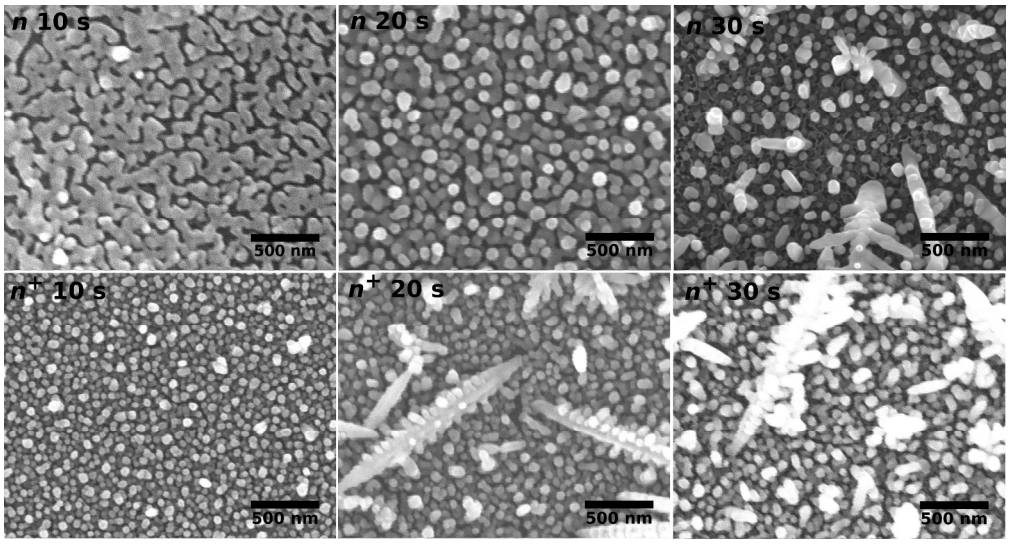

Figure 4. Silver seeds deposited on silicon substrates after 10'', 20'' and 30'' of MACE etching (CONCENTRATION). On the top: n-doped substrate (resistivity 5-10 Ohm cm); on the bottom: n+-doped substrate (resistivity 0.003 Ohm cm).

1089x581mm (100 x 100 DPI)

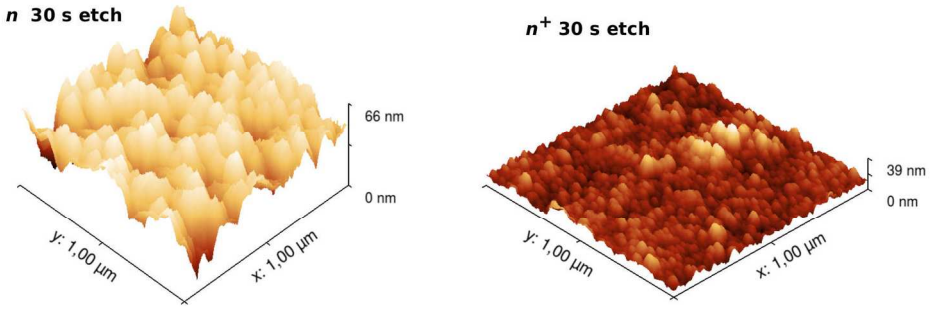

Figure 5. AFM images (no-contact mode) of silicon surfaces, after 30" of MACE etching and silver removal by HNO3 etching (see text). On the left: the n-doped substrate shows the initial formation of vertical structures, whose length can be estimated of 30-50 nm. On the right: the n+-doped substrate presents a rough surface, with a standard deviation of about 4 nm.

473x204mm (100 x 100 DPI)